COO-3072-29
SESSION A_3
Conf-740713--18

Paper submitted to the XVII International Conference on High Energy Physics, Imperial College, London, 1-10 July 1974

32334

Atomic Number Dependence of Hadron Production at Large Transverse Momentum in 300 GeV Proton-Nucleus Collisions*

J. W. Cronin, H. J. Frisch, and M. J. Shochet
The Enrico Fermi Institute, University of Chicago, Chicago, Illinois 60637

and

J. P. Boymond, R. Mermod†, P. A. Piroué, and R. L. Sumner
Department of Physics, Joseph Henry Laboratories
Princeton University, Princeton, New Jersey 08540

ABSTRACT

In an experiment at the Fermi National Accelerator Laboratory we have compared the production of large transverse momentum hadrons from targets of W, Ti, and Be bombarded by 300 GeV protons. The hadron yields were measured at 90° in the proton-nucleon c.m. system with a magnetic spectrometer equipped with 2 Cerenkov counters and a hadron calorimeter. The production cross-sections have a dependence on the atomic number A that grows with $p_\perp$, eventually leveling off proportional to $A^{1.1}$.

DISCLAIMER

There has recently been a great deal of interest in the interaction of high-energy hadrons with nuclear matter[1]. We present here data on the production of high transverse momentum hadrons by 300 GeV protons from targets of Be, Ti, and W.

These data were obtained in the Proton area of the Fermi National Accelerator Laboratory (NAL) with a focusing magnetic spectrometer viewing the target at an angle of 77 mrad in the laboratory. For relativistic particles this corresponds to an angle in the proton-nucleon c.m. of 88°. Two 86-ft-long gas Cerenkov counters were used to identify the secondary particles as $\pi^{\pm}$, $K^{\pm}$, $p^{\pm}$, $d^{\pm}$. The apparatus is described in detail elsewhere[2]. The targets were chosen to cover a wide range in atomic number ($\bar{A}$). In order that in the comparison no correction would be necessary due to secondary interactions in the target, the length of each 1/4 in. diameter target was chosen to be the same number of interaction lengths. Using absorption cross sections[3] of 227 mb, 690 mb, and 1635 mb for Be, Ti, and W, we chose the respective target lengths to be 3.14 in., 2.23 in., and 0.85 in. In each of these targets 20% of the primary beam interacted.

The three targets were mounted side by side on a remotely controlled X-Y stage. In order to minimize systematic effects in the target comparison, such as those due to fluctuations in beam conditions, runs at a given $p_{\perp}$ were taken with all three targets in quick succession. All other conditions, such as magnet settings, the Cerenkov counter pressures, etc., remained unchanged.

The run-to-run targetting efficiency and normalization were determined by a three counter scintillator telescope looking at the

target at 90° in the laboratory. The overall normalization for each target was determined by calibrating this 90° monitor with a secondary emission monitor in the primary proton beam 20 ft. upstream of the target.

The measured invariant cross sections per nucleus[4], $Ed\sigma_A/d^3p$ for pion production for Beryllium are presented in Table I. Kaon, proton, and deuteron cross sections are presented as ratios to the pion cross section. The formula used for calculating the cross sections is

$$E\frac{d\sigma_A}{d^3p} = \frac{A}{\rho L N_o}\ \frac{1.15Y}{p^2\ \Delta\Omega\ \Delta P/P}\ \exp(N_o\rho L\sigma_{abs}/A)$$

where A, ρ, σ_{abs}, and L are the atomic number, density, absorption cross section, and length, respectively, of the target; N_o is Avogadro's number, Y is the measured pion yield per incident proton, $\Delta\Omega\Delta P/P = 1.7 \times 10^{-6}$ sr is the spectrometer acceptance, P is the secondary momentum in the laboratory, and the 1.15 is the correction for absorption in the spectrometer.

The invariant cross sections per nucleus for hadron production from targets of Ti and W are presented as ratios to the Be cross sections in Table II. One sees that the ratios rise with increasing $p_\perp$, indicating a stronger dependence on A at larger $p_\perp$.

Figure 1 shows the ratio of the invariant cross sections per nucleus for π^+ and p production from Ti and W compared to those from Be, plotted versus the atomic number A. The approximately linear relationship of the plotted cross sections implies a power law dependence on A. One sees that the A dependence gets stronger with increasing $p_\perp$. Using this

figure, one can also extrapolate to the proton-nucleon cross section; however, because the nuclear cross sections contain both p-n and p-p collisions, one cannot directly extract the p-p cross sections.

Figure 2 shows the power n as a function of $p_\perp$ derived by assuming that the cross section per nucleus for π^- production is proportional to A^n. The values of n derived from comparing the two nuclei are in remarkable agreement, showing that for all values of $p_\perp$ between 0.76 and 6.10 GeV/c the assumption of a power law A^n works well. One sees that the value for n rises steeply with $p_\perp$, leveling off near $n = 1.1$ at $p_\perp \approx 4$ GeV/c.

The π^+ cross-sections display a similar behavior, but the proton, anti-proton, and $K^\pm$ ratios are appreciably steeper as a function of $p_\perp$. This has the consequence that the proton to pion ratio, for example, is smaller with a Be target than with a W target. Figure 3 shows the p/π^+ and $\bar{p}/\pi^-$ ratios from both Be and W targets--one sees that the qualitative features observed[2] with W still obtain with Be.

We would like to express our appreciation to the staff of the Fermi National Accelerator Laboratory, and especially to that of the Proton Section for their support. Finally, one of us (R.M.) wishes to thank NAL for its hospitality and support.

REFERENCES

*Work supported by the National Science Foundation and the U. S. Atomic Energy Commission.

†On leave at NAL from the University of Geneva.

1. See, for example, K. Gottfried, CERN preprint, Ref.-TH 1735-CERN (1973) (to be published).

E. Lehman and G. A. Winbow, P. L. 46B, 375 (1973).

K. Gottfried, P.R.L. 32, 957 (1974)

Also data from an experiment at lower $p_\perp$ at 24 GeV is described in T. Eichten et al. Nucl. Phys. 44, 333 (1972).

2. J. W. Cronin et al., P.R.L. 31, 1426 (1973).

3. Bellatini et al., Nucl. Phys. 79, 609 (1966).

4. No one should be confused by the transformation from invariant cross section per nucleus to invariant cross section per effective nucleon. For a thin target, the number of nuclei per cm^2 is $N_o \rho L/A$, while the number of effective nucleons seen by an incoming proton is $\frac{\sigma_{abs}}{\sigma_p} (N_o \rho L/A)$ where σ_{abs} is the absorption cross section for the nucleus and σ_p is the total p-p cross section.

Therefore, to compute the invariant cross section per effective nucleon, divide the invariant cross section per nucleus by a factor of 5.68, 17.3, or 40.9 for Be, Ti, or W respectively.

TABLE CAPTIONS

Table I. Invariant cross sections for pion production per nucleus in p-Be collisions as a function of $p_\perp$. Also shown are the ratios of K, p, and d production to π production. At each momentum the upper line is for positive particle production (e.g., π^+, K^+/π^+, etc.) and the bottom line for negative (π^-, K^-/π^-, etc.)

Table II. The ratios of invariant cross sections for the production of $\pi^\pm$, $K^\pm$, $p^\pm$, and $d^\pm$ from Ti and W relative to the production from Be as a function of $p_\perp$. At each momentum the upper line is for positive particle production (e.g., π^+, K^+, p,d) and the lower line is for negative (π^-, K^-, $\bar{p}$, $\bar{d}$).

FIGURE CAPTIONS

Figure 1. The ratio of invariant cross sections per nucleus for π^+ and p production from W and Ti compared to those from Be, plotted vs. atomic number A. Data are shown for three different values of $p_\perp$: $p_\perp$ = 0.79, 2.29, and 5.34 GeV/c.

Figure 2. The value of n derived from comparing π^- production from Ti and W to that from Be, assuming that the invariant cross section depends on the atomic number A via a power law, $E \frac{d\sigma}{d^3p} \propto A^n$, plotted versus the transverse momentum $p_\perp$.

Figure 3. The ratio of proton to π^+ and $\bar{p}$ to π^- production vs. $p_\perp$ from proton-Be and proton-W collisions at 300 GeV.

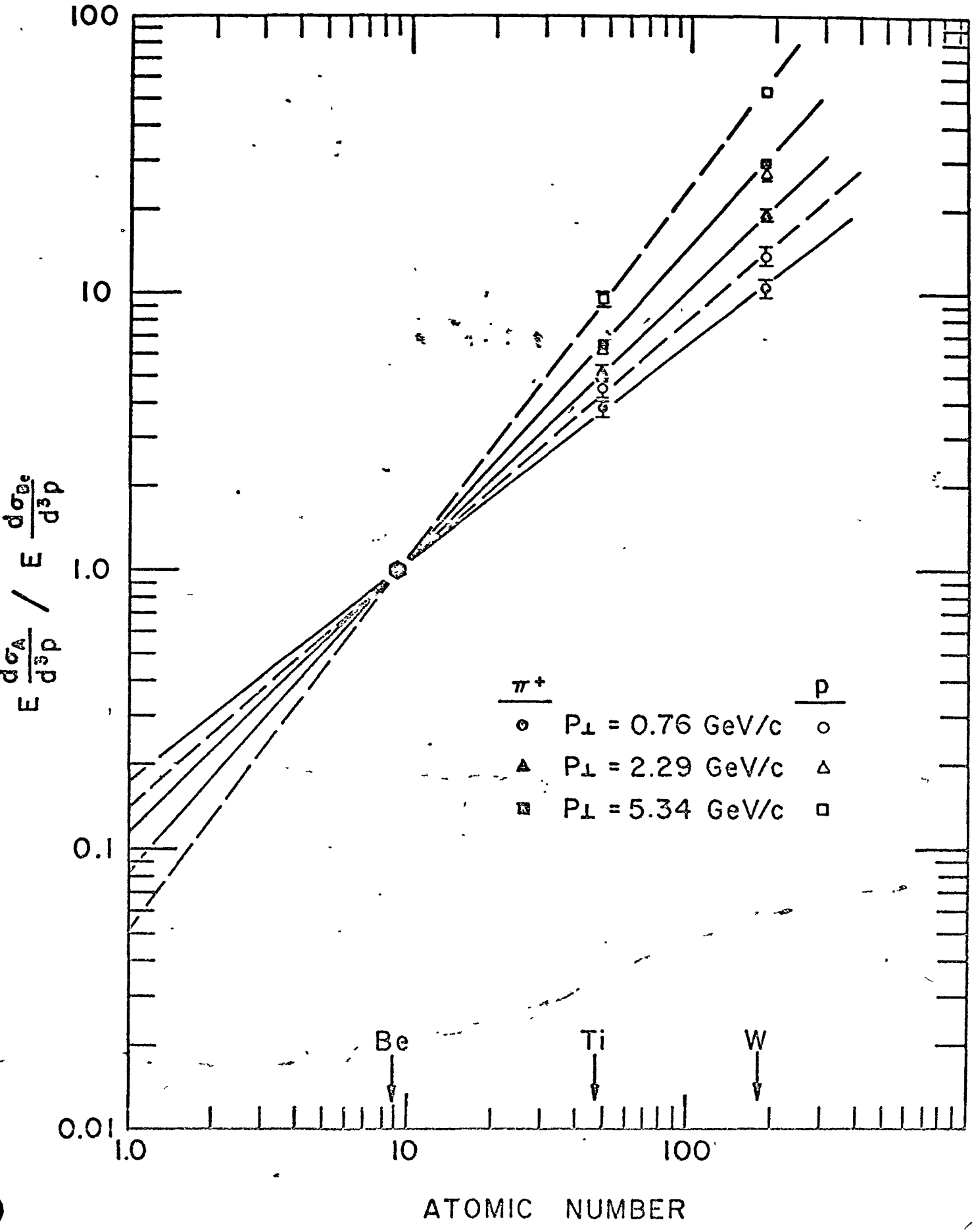
100
10
1.0
0.1
0.01
1.0
10
100
$E\frac{d\sigma_A}{d^3p} / E\frac{d\sigma_{Be}}{d^3p}$
ATOMIC NUMBER
Be
Ti
W
π^+
p
$P_\perp$ = 0.76 GeV/c
$P_\perp$ = 2.29 GeV/c
$P_\perp$ = 5.34 GeV/c

FIGURE 1

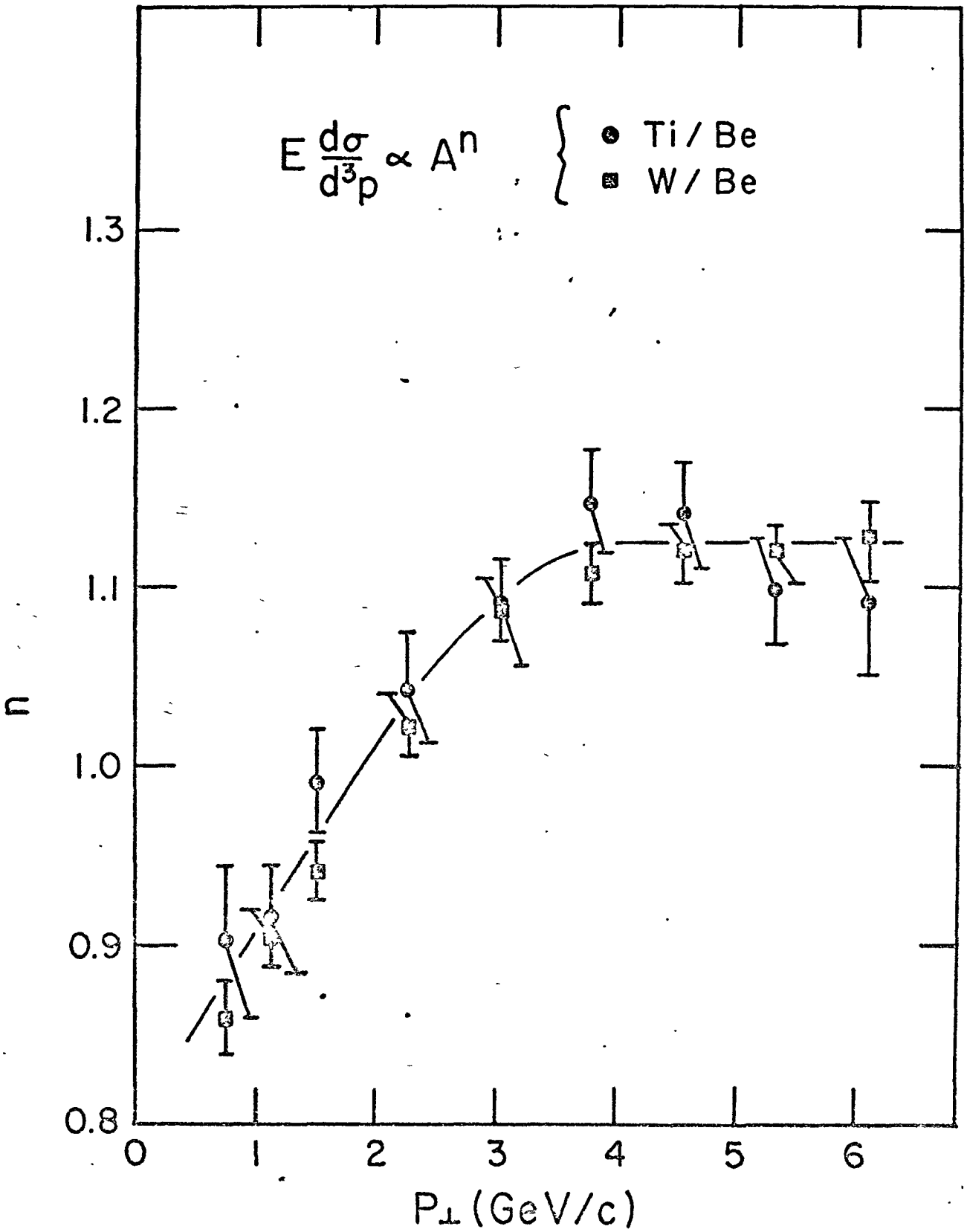
$E\frac{d\sigma}{d^3p} \propto A^n$
Ti / Be
W / Be
1.3
1.2
1.1
1.0
0.9
0.8
n
0
1
2
3
4
5
6
$P_\perp$ (GeV/c)

FIGURE 2

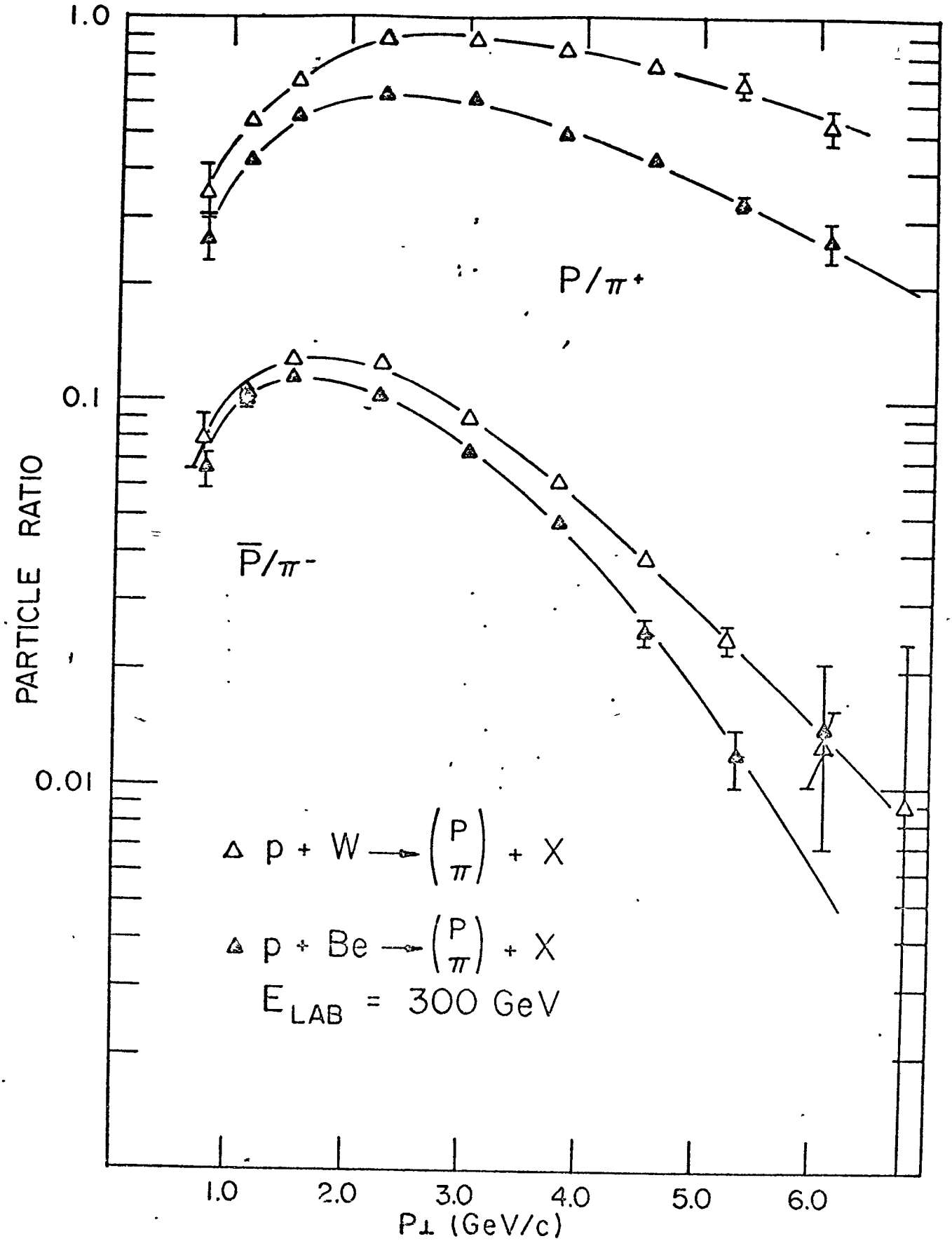
1.0
0.1
0.01
PARTICLE RATIO
P/π+
P̄/π-
Δ p + W → (P/π) + X
Δ p + Be → (P/π) + X
E_LAB = 300 GeV
1.0
2.0
3.0
4.0
5.0
6.0
P⊥ (GeV/c)

FIGURE 3

$p_\perp$ (GeV/c)	$Ed\sigma(\pi)/d^3p$	K/π	p/π	d/π
0.76	$(1.27\pm.18)$ X 10^{-26} $(1.02\pm.14)$	$.18\pm.04$ $.12\pm.02$	$.26\pm.03$ $.066\pm.007$	
1.14	$(1.74\pm.12)$ X 10^{-27} $(1.44\pm.10)$	$.269\pm.016$ $.166\pm.011$	$.421\pm.014$ $.100\pm.004$	
1.53	$(2.54\pm.18)$ X 10^{-28} $(2.17\pm.15)$	$.310\pm.018$ $.192\pm.013$	$.552\pm.017$ $.114\pm.005$	
2.29	$(1.03\pm.07)$ X 10^{-29} $(.82\pm.06)$	$.398\pm.023$ $.232\pm.014$	$.622\pm.019$ $.101\pm.005$	$(2.0\pm.2)$ X 10^{-3} $(1.4\pm.2$ X 10^{-4}
3.05	$(4.83\pm.34)$ X 10^{-31} $(4.02\pm.28)$	$.447\pm.026$ $.238\pm.014$	$.610\pm.020$ $.073\pm.004$	$(2.3\pm.2)$ X 10^{-3}
3.81	$(3.18\pm.22)$ X 10^{-32} $(2.65\pm.19)$	$.457\pm.028$ $.189\pm.012$	$.494\pm.018$ $.048\pm.003$	$(1.9\pm.2)$ X 10^{-3}
4.58	$(2.16\pm.15)$ X 10^{-33} $(1.97\pm.14)$	$.510\pm.031$ $.162\pm.010$	$.424\pm.017$ $.025\pm.002$	$(2.3\pm.6)$ X 10^{-3}
5.34	$(2.20\pm.15)$ X 10^{-34} $(1.73\pm.12)$	$.470\pm.029$ $.106\pm.008$	$.330\pm.014$ $.012\pm.002$	
6.10	$(2.58\pm.18)$ X 10^{-35} $(1.66\pm.14$	$.377\pm.043$ $.079\pm.016$	$.263\pm.031$ $.014\pm.007$	
6.87	$(1.9\pm.3)$ X 10^{-36}	$.099\pm.031$	$.009\pm.009$	

Table I

$p_\perp$ (GeV/c)	σ_{Ti}/σ_{Be} π	K	p	d	σ_W/σ_{Be} π	K	p	d
0.76	3.84±.27 4.52±.32	4.67±.33 5.32±.38	4.54±.32 5.35±.38		10.5±.7 13.4±.9	12.4±.9 15.3±1.1	13.8±1.0 15.6±1.1	
1.14	4.85±.24 4.61±.23	5.26±.27 5.06±.25	5.54±.28 4.83±.24		14.0±.7 15.3±.8	15.9±.8 18.5±.9	17.7±.9 16.0±.8	
1.53	4.73±.24 5.25±.26	5.39±.27 5.61±.28	5.45±.27 5.10±.26		15.6±.8 17.1±.8	19.0±.9 18.1±.9	19.5±.9 19.0±1.0	
2.29	5.22±.26 5.71±.29	5.59±.28 5.80±.29	6.44±.32 6.47±.32	10.2±1.1 7.3±1.3	19.3±.9 21.8±1.1	21.5±1.1 22.7±1.1	27.1±1.4 25.2±1.3	45.±6. 22.±4.
3.05	6.25±.31 6.13±.31	6.43±.32 6.03±.30	8.07±.40 7.26±.36	11.7±1.5	24.6±1.2 26.6±1.3	27.5±1.4 27.3±1.4	34.1±1.7 32.5±1.6	71.±9.
3.81	6.50±.33 6.80±.34	6.82±.39 7.60±.38	8.86±.45 9.20±.46	13.7±2.0	27.2±1.4 28.1±1.4	33.0±1.7 34.0±1.7	46.1±2.3 36.2±1.8	74.±10.
4.58	7.08±.35 6.71±.34	7.23±.36 8.07±.40	9.91±.50 10.4±.52	13.2±4.2	29.2±1.5 29.3±1.5	30.9±1.5 34.4±1.7	50.3±2.5 50.6±2.5	57.±16.
5.34	6.50±.38 6.25±.31	7.15±.36 9.06±.46	9.54±.48 12.6±2.6		29.5±1.5 29.2±1.5	35.2±1.8 43.9±2.2	53.1±2.7 51.4±10.8	
6.10	6.41±.64 6.16±.39	9.2±1.3 7.9±1.9	8.8±1.4 6.3±4.3		25.0±2.5 29.8±1.9	34.5±5.0 45.7±10.7	34.3±5.0 26.0±15.0	

Table II